論文 / 著書情報
Article / Book Information

Title	Scaling up microdroplet production with post-array devices
Authors	Shuzo Masui, Yusuke Kanno, Takasi Nisisako
Citation	Biomicrofluidics, Vol. 19, ,
Pub. date	2025, 5
Note	This article may be downloaded for personal use only. Any other use requires prior permission of the author and AIP Publishing. This article appeared in Shuzo Masui, Yusuke Kanno, Takasi Nisisako; Scaling up microdroplet production with post-array devices. Biomicrofluidics. 28 May 2025; 19: 031303 and may be found at https://doi.org/10.1063/5.0270507.
Note	This file is author (final) version.

Scaling up microdroplet production with post-array devices

Shuzo Masui,[1] Yusuke Kanno,[2] Takasi Nisisako[2,a)]

AFFILIATIONS

[1] Department of Precision Engineering, Graduate School of Engineering, the University of Tokyo, Bunkyo-ku, Tokyo, 113-8656, Japan

[2] Laboratory for Future Interdisciplinary Research of Science and Technology, Institute of Integrated Research, Institute of Science Tokyo, 4259 Nagatsuta-cho, Midori-ku, Yokohama, 226-8501, Japan

[a)]**Author to whom correspondence should be addressed**: *nisisako.t.aa@m.titech.ac.jp*. Tel.: +81-45-924-5092

ABSTRACT

Microfluidic systems capable of generating uniform droplets are gaining attention in food, cosmetics, biochemical, and materials applications. While conventional shear- or interfacial tension-driven nozzle devices can generate highly monodisperse droplets (CV < 5%), their scalability is limited by complex flow designs and clogging. Post-array devices have recently emerged as a high-throughput alternative, producing quasi-monodisperse droplets (CV > 12%) by sequentially breaking larger droplets using micro-post structures. These devices offer shear-dependent tunability of droplet sizes, greater resistance to clogging, and scalability. Notably, droplet size is strongly influenced by the dispersed phase fraction, enabling potential decoupling of droplet size and dispersed phase fraction. This study reviews the principles and performance of post-array devices, compares them with other droplet generation methods, and examines their similarities to droplet splitting in T-junctions and premix membrane emulsification. Challenges such as improving droplet uniformity and miniaturization are also discussed to highlight the potential of post-array systems for practical emulsification applications.

I. INTRODUCTION

Microfluidic droplet generators are increasingly being explored for applications in fields such as food processing,[1] cosmetics,[2] biochemistry,[3] and materials science[4] due to their ability to produce droplets of precisely controlled size and composition while integrating droplet generation with multifunctional analytical capabilities.[5] These devices are generally of two types: shear-based devices, such as T-junction and flow focusing devices, and interfacial tension-driven devices, such as step emulsification devices.[6–8] While both approaches can produce highly monodisperse droplets with a coefficient of variation (CV) of less than 5% in diameter at a single nozzle, scaling up production requires parallelization of droplet generation nozzles. However, this presents challenges such as the complex design and fabrication of fluid distribution channels to ensure uniform flow delivery, along with an increased risk of clogging.[9]

Although precise droplet size control is essential in many applications, microfluidic devices that prioritize robustness against clogging and ease of use are also valuable for specific purposes. For example, they are employed in the preliminary emulsification of double emulsions for drug delivery,[10] in the generation of droplets containing beads or cells that are prone to clogging,[11] and in biochemical analysis techniques that utilize polydisperse droplets.[12,13] Additionally, recent advances in microfluidic sorting technologies have enabled the selective isolation of target droplets from polydisperse droplets.[14] In such applications, ease of operation and device durability often take precedence over achieving highly uniform droplet sizes. This growing diversity in microfluidic emulsification requirements is driving the development of alternative droplet generation technologies.

Recently, post-array devices have gained significant interest as an innovative microfluidic approach to produce quasi-monodisperse droplets at high throughput. These devices generate small droplets by progressively breaking up larger droplets using regularly arranged micro-post structures.[15–18] Unlike conventional nozzle-based microfluidic systems, post-array devices employ a distinct droplet breakup mechanism and offer unique advantages in scalability and robustness. In this paper, we introduce the basic principles of post-array devices, review recent research findings, and compare their performance with other high-throughput droplet generation techniques. Finally, we discuss the remaining challenges and future prospects associated with these devices.

II. DROPLET GENERATION WITH POST-ARRAY DEVICES: FUNDAMENTALS, MECHANISM, AND FUTURE PROSPECTS

A. Key features and advantages of post-array devices

The post-array device is a relatively new microfluidic droplet generator, first introduced by Amstad *et al*. in 2014 (Fig. 1a).[15] In these devices, the dispersed and continuous phases are introduced into the post-array region either as a premixed coarse emulsion[15] or through a sheath flow configuration (Fig. 1b).[16–18] As the fluid passes through the post-array, larger droplets are repeatedly fragmented into smaller ones, producing emulsions with size uniformity ranging from quasi-monodisperse to polydisperse levels at high throughput.

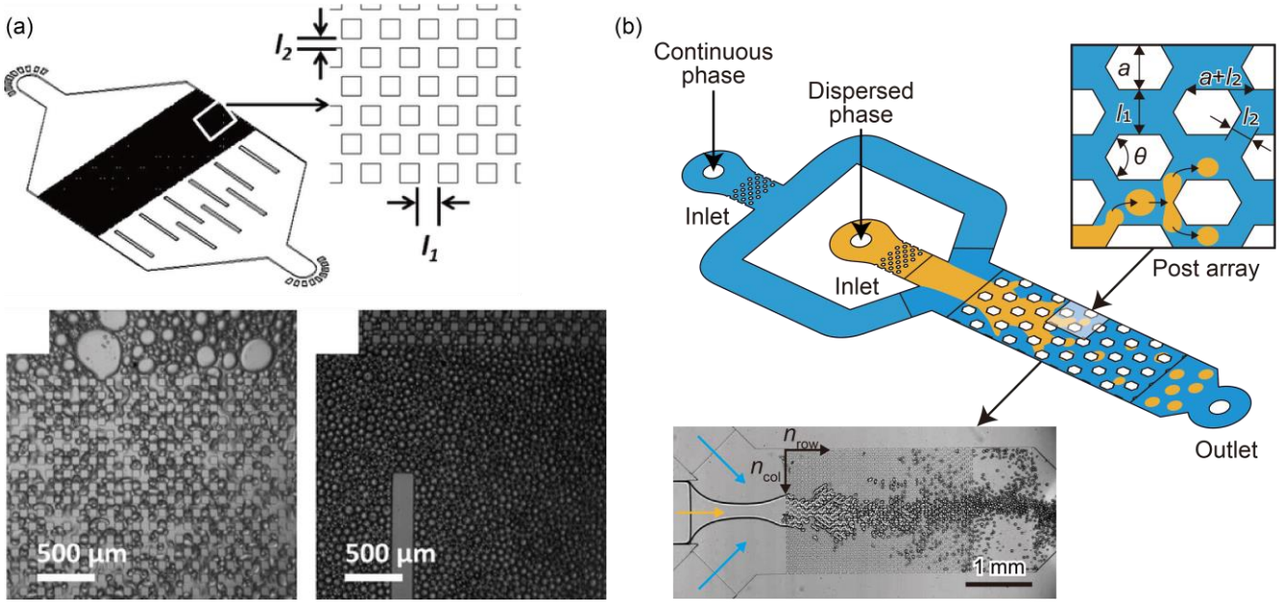

FIG. 1. Schematic of post-array devices and microscope images of droplet generation. (a) Premix emulsion feeding system. Reproduced with permission from Amstad *et al.*, Lab Chip **14**, 705 (2014). Copyright 2014 Royal Society of Chemistry.[15] (b) sheath flow configuration. Reproduced with permission from Masui *et al.*, Lab Chip **23**, 4959 (2023). Copyright 2023 Royal Society of Chemistry.[16]

A key feature of post-array devices is their ability to tune droplet size within a given device geometry by varying flow-induced shear forces. Although shear-driven droplet breakup is common, the breakup mechanism in post-array devices is fundamentally different from conventional single nozzle-based shear-driven systems. Unlike nozzle-based microfluidics, where droplets are formed individually at discrete nozzles, post-array devices allow simultaneous droplet formation at multiple and varying points throughout the post-array, significantly increasing throughput and scalability.

One of the major advantages of post-array devices is their ease of high throughput. Their design eliminates the need for complex parallelized channel networks, simplifying fabrication and allowing for large-scale production without the need for precisely engineered flow resistances or complex three-dimensional channel layouts.[19] Amstad *et al*. demonstrated the high-throughput production of poly(dimethylsiloxane) (PDMS) microparticles with a mean diameter of 20 µm and a CV of 20% (Fig. 2a) at a flow rate of 50 mL/h using a 40-row × 300-column post-array device (dimensions: 6 mm × 24 mm × 5 mm).[15] This work highlights the potential of post-array devices for high-throughput droplet generation using a simple two-layer PDMS chip.

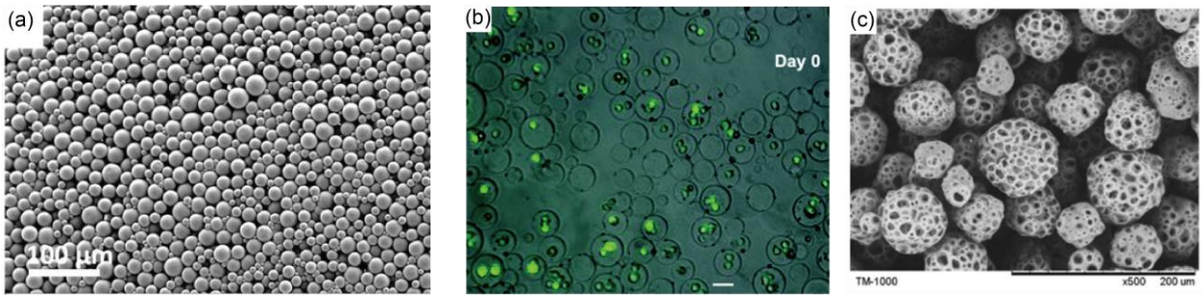

FIG. 2. Particles synthesized from various precursor droplets generated by post-array and their combined device. (a) PDMS beads. Reproduced with permission from Amstad *et al.*, Lab Chip **14**, 705 (2014). Copyright 2014 Royal Society of Chemistry.[15] (b) Poly(ethylene glycol) hydrogel beads encapsulating fluorescent labeled MDA-MB231 cell. Reproduced with permission from Akbari *et al.*, Lab Chip **17**, 2067 (2017). Copyright 2017 Royal Society of Chemistry.[17] (c) PLGA microparticle prepared by combination of post-array and cross-flow device. Reproduced with permission from Yeh *et al.*, Microfluid. Nanofluidics **27**, 47 (2023). Copyright 2023 Springer Nature.[18]

Another unique feature of post-array devices is the strong influence of the dispersed phase fraction on droplet size. Masui *et al*. demonstrated that the dispersed phase fraction, defined as the volume ratio of the dispersed phase flow rate to the continuous phase flow rate, plays a critical role in determining the final droplet size.[16] This effect was quantified by evaluating the effective shear force, which depends on the emulsion viscosity, a property that increases with the dispersed phase fraction.[20,21] This dependence suggests the potential for independent control of droplet size and dispersed phase fraction, a capability that distinguishes post-array devices from many conventional microfluidic systems. For example, increasing the dispersed phase fraction while decreasing the total flow rate can maintain a constant effective shear force and preserve droplet size. Conversely, decreasing the dispersed phase fraction while increasing the total flow rate can achieve a similar effect. These characteristics make post-array devices particularly advantageous for applications requiring independent control of droplet size and volume fraction.

Post-array devices also exhibit a high degree of robustness against clogging, making them particularly suitable for applications where channel blockage is a major challenge. Unlike nozzle-based microfluidic droplet generators, which rely on discrete channels that are highly susceptible to blockage, post-array devices maintain functionality even in the presence of localized clogging. This is because unaffected regions of the post-array continue the droplet splitting process, ensuring sustained production efficiency. Akbari *et al*. successfully produced hydrogel beads with an average diameter of 45 μm encapsulating breast cancer cells (MDA-MB231) (Fig. 2b),[17] demonstrating the potential of post-array devices to produce cell-encapsulated droplets at high throughput while maintaining robustness to clogging.

B. Mechanisms of droplet breakup in post-array devices

While the breakup dynamics of nozzle-based droplet generators,[6] constricted microchannels,[22] and single-droplet splitting in T-junctions[23–26] have been extensively studied, those of post-array devices have only recently been investigated. Although the hydrodynamics of single-droplet splitting in T-junctions has been extensively studied,[23–26] these principles had not previously been applied to the multi-droplet breakup observed in post-array devices, largely due to the challenges associated with quantifying shear forces in such systems. To address this issue, Masui *et al*. demonstrated that the flow-induced shear force driving the droplet breakup within the post-array can be accurately evaluated using the effective capillary number,[16] $Ca_{eff} = \eta_e U / \gamma$, where η_e, U, and γ represent the emulsion viscosity,[20,21] fluid velocity, and interfacial tension, respectively. In general, the emulsion viscosity η_e increases rapidly with the volume fraction of the dispersed phase relative to the continuous phase.[20,21] The use of Ca_{eff} enabled the adaptation of well-established single-droplet breakup theories in T-junctions to elucidate the breakup mechanisms in post-array devices.

Masui *et al*. classified droplet breakup in post-array devices into two distinct modes based on Ca_{eff} (Fig. 3a)[16] At low Ca_{eff} (< 0.003), the obstruction mode dominates, where interfacial tension primarily governs breakup, and steric hindrance imposed by the post-array dictates droplet size, making it independent of flow rate (Fig. 3b). In contrast, as Ca_{eff} increases, the shear-induced mode emerges, where shear forces become the dominant factor, leading to droplet size reduction that follows a power-law dependence on Ca_{eff} (Fig. 3c). This behavior closely resembles the droplet splitting dynamics observed in T-junctions.[25,26] However, at excessively high Ca_{eff} (> 0.03), satellite droplet formation increases, significantly degrading droplet size uniformity, similar to observations in T-junction splitting.[16,23] Furthermore, while the viscosity ratio between the dispersed and continuous phases has little impact on the average droplet size, it significantly influences droplet uniformity. Specifically, increasing the viscosity of the dispersed phase reduces the CV under low shear conditions (Ca_{eff} < 0.02), thereby enhancing monodispersity.[16] Therefore, maintaining Ca_{eff} within an optimal range and appropriately adjusting the viscosity ratio are essential for precisely tuning droplet size while achieving a low CV in the final product.

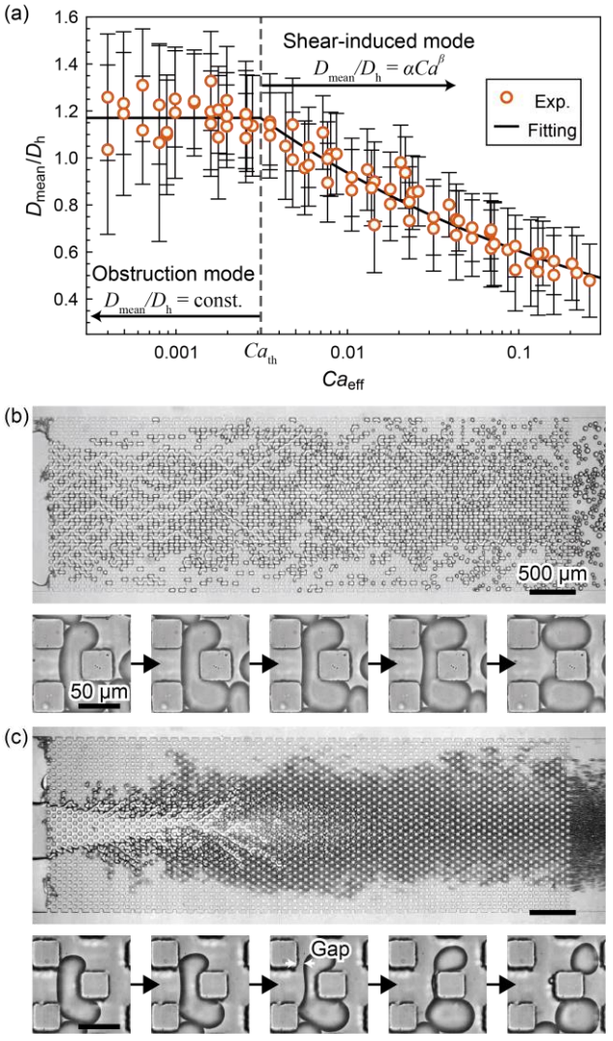

FIG. 3. Two droplet generation modes governed by the magnitude of shear force, along with their characteristic differences. (a) Variation of the normalized mean droplet diameter D_{mean}/D_h as a function of Ca_{eff}, with error bars representing the standard deviation. (b, c) Microscope images of droplet generation in (b) obstruction mode (Ca_{eff} = 0.003) and (c) shear-induced mode (Ca_{eff} = 0.16). Time-sequenced magnified views of droplet breakup are shown below each image, with time intervals of (b) 2 ms and (c) 0.3 ms. Reproduced with permission from Masui *et al.*, Lab Chip **23**, 4959 (2023). Copyright 2023 Royal Society of Chemistry.[16]

Post-array devices share strong similarities with both T-junction droplet splitting and premix membrane emulsification (PME). The two breakup modes—obstruction and shear-induced—observed in post-array devices are consistent with those identified in single-droplet splitting at T-junctions.[16,25,26] In addition, both T-junction droplet splitting and post-array devices exhibit the formation of a gap between the droplet and the channel walls, as well as an increase in satellite droplet size under high shear conditions.[16,24] Similarly, in PME, droplet breakup has

been observed when the capillary number exceeds a critical threshold of approximately 0.003 in a silicon-based microfabricated device,[28] which aligns well with the transition from obstruction to shear-induced mode at Ca_{eff} = 0.003 in post-array devices.[16] Furthermore, droplet size in post-array devices ranges from approximately 0.76 to 1.34 times the hydraulic diameter between posts,[16] which closely matches the PME droplet-to-pore size ratio of 0.7 to 1.5.[29]

Given these similarities, post-array devices can be regarded as a microfluidic implementation of 2D membrane emulsification. The shared characteristics between PME, T-junction droplet splitting, and post-array devices suggest that theoretical and experimental insights from single-droplet breakup studies can be used to optimize post-array geometries and design engineered membranes for PME.[30] Ultimately, post-array devices may serve as a bridge between well-characterized single-droplet breakup dynamics and the complex yet practical emulsification mechanisms employed in porous membranes.

Post-array design involves numerous parameters—including post size, shape, and spacing—that influence both droplet size and uniformity. However, because droplet characteristics are also affected by the operating Ca_{eff} and the droplet generation mode, it is challenging to isolate the effects of post design. Although Amstad *et al*. reported droplet size and CV across various post designs under sufficiently high Ca (>0.03) conditions, generalized design rules for post-arrays remain unclear.[15] Masui *et al*. qualitatively evaluated the effects of post design and viscosity ratio by curve fitting, deriving coefficients that describe droplet size in the obstruction mode and the scaling behavior with Ca_{eff}.[16] Their results showed that increasing post spacing leads to larger droplet sizes in the steric hindrance mode, while sharper post tips yield smaller droplets. However, for droplet uniformity, the operating Ca_{eff} remains the dominant factor, and further studies are needed to elucidate the specific role of post design.

The role of local flow dynamics in droplet breakup within post-array devices has been investigated. In sheath-flow-type post-array devices, an increase in the droplet fraction in the central region of the array has been observed (Fig. 3c). Although Masui *et al.* performed a detailed analysis of droplet size and velocity distributions across the direction perpendicular to the flow, no significant variation in droplet size was detected.[16] This apparent stability is attributed to a compensatory mechanism: as the local fraction of the dispersed phase increases, the emulsion viscosity rises, which subsequently lowers the local flow velocity. As a result, the shear stress—proportional to the pressure gradient—remains effectively constant, suppressing fluctuations in droplet size.

Wettability also plays a critical role in droplet breakup within post-array devices. As in other microfluidic droplet generators, hydrophobic post arrays are typically used to produce water-in-oil (W/O) droplets,[15,17,18] while hydrophilic post arrays are employed for oil-in-water (O/W) droplets.[15,16] However, heterogeneities in surface wettability may adversely affect droplet size uniformity. For example, a numerical study demonstrated the emergence of asymmetric splitting and even non-splitting modes in bifurcated channels with differing wettability.[27] If a similar mechanism operates within post-array systems, surface treatment heterogeneities could promote asymmetry in droplet breakup, leading to increased variation in droplet size.

C. Comparative analysis of high-throughput droplet generators

The performance of post-array devices compared with other high-throughput microfluidic droplet generators and industrial membrane emulsification methods is summarized in Table 1. This comparison considers key parameters such as droplet generation mechanisms, droplet size, CV, and maximum dispersed phase throughput for six technologies: post-array devices (premix and sheath flow configurations), flow focusing, step emulsification, porous devices, and PME. The maximum permeation flux of the dispersed phase was calculated using the entire device footprint for step-emulsification and flow focusing devices, while only the area of the post-array or porous membrane was considered for post-array and PME-based systems.

Table 1. Comparison between various high-throughput droplet generators

Method	**Post-array (premix)**	**Post-array (sheath flow)**	**Flow focusing**	**Step emulsification**	**Microfluidic porous device**	**PME**
Droplet generation mechanism	Droplet breakup	Droplet breakup	Shear force driven	Interfacial tension driven	Interfacial tension driven	Droplet breakup
Device dimension	2D	2D	2D	3D	3D	3D
Droplet size [μm]	16–45	8–65	22.5–37.5	87	7.0–75	0.1–260
CV [%]	13–22	12–50	3.3	2	10.9–20.6	12–31
Maximum flux of dispersed phase [L h^{-1} m^{-2}]	520	2100[18]	930	2600	600	200000[33]
Reference	15	16–18	19	31	32	29, 33

Post-array devices can generate droplets in the size range of 8 to 65 μm, with the best CV values for droplet diameter at 12–13%, regardless of whether the liquid feeding method is premixed or sheath flow.[15–18] The highest throughput for post-array devices was demonstrated by Yeh *et al*., who achieved W/O droplet generation for the pre-emulsification of poly(lactic-co-glycolic acid) (PLGA) particles (Fig. 2c) at a rate of approximately 2100 L h^{-1} m^{-2}.[18] In contrast, flow focusing devices have been shown to produce highly monodisperse droplets. Yadavali *et al*. successfully produced hexadecane droplets with a diameter of 22.5 μm and a CV of 3.3% at a maximum throughput of 930 L h^{-1} m^{-2} using a silicon and glass device with 10260 nozzles.[19] Similarly, Kobayashi *et al*. utilized a 24,772-nozzle microchip fabricated on a silicon-on-insulator substrate to produce *n*-tetradecan O/W droplets with a diameter of 87 μm and a CV of less than 2% at a rate of 2600 L h^{-1} m^{-2}.[31] Recently, Mashiyama *et al*. developed a microfluidic porous device consisting of an inverse colloidal crystal structure in a microchannel using polymer

particles as porogens, which allowed the production of W/O droplets with a diameter of 33.1±3.6 μm (i.e., CV of 10.9%) at a throughput of 600 L h^{-1} m^{-2}.[32] PME, which is widely employed in industrial applications, allows the generation of droplets ranging from 100 nm to several hundred micrometers, depending on the membrane pore size.[29] The minimum CV for PME is approximately 12%, with a maximum throughput of approximately 200000 L h^{-1} m^{-2}.[33]

A comparative analysis of these technologies highlights both the advantages and limitations of post-array devices. Flow-focusing devices are particularly effective at producing highly monodisperse droplets with tunable sizes; however, achieving uniform flow distribution in these systems requires carefully designed flow resistances and complex microchannel fabrication. In contrast, post-array devices, along with step emulsifiers and porous devices, offer easier scalability and greater robustness against clogging by encapsulated materials such as cells, reducing the need for complicated designs. Step emulsifiers and porous devices, which rely on interfacial tension-driven emulsification, are inherently limited to producing droplets larger than the pore diameter, limiting their capacity for further droplet size reduction. Conversely, post-array devices, PME, and flow-focusing devices, which utilize shear forces to generate droplets, can produce droplets smaller than the nozzle size or pore diameter. This capability suggests that post-array devices are particularly well suited for the large-scale production of quasi-monodisperse droplets containing encapsulated materials prone to clogging, as well as for fine droplet generation in high-throughput applications.

D. Challenges in post-array devices: droplet uniformity and size reduction

Despite recent advances, two major challenges remain for post-array devices: improving droplet uniformity and achieving smaller droplet sizes. Even when utilizing highly uniform post-array structures or feeding droplets with a CV below 5%,[15] the minimum achievable CV remains at 12%, comparable to that of PME, suggesting an intrinsic limit to uniformity. It has been observed that the droplet size distribution in post-array devices at $Ca_{eff} > 0.03$ can be well described as a sum of two normal distributions, suggesting that multiple droplet breakup processes may be occurring simultaneously.[16] Addressing this issue requires a deeper investigation into the underlying mechanisms governing droplet size variation in post-array devices, which are likely to share similarities with PME. One promising approach is the serial integration of post-array devices with deterministic lateral displacement (DLD) technology,[34] which uses post-arrays with designed lateral shifts to selectively separate smaller or larger particles. Several studies have demonstrated that integrating nozzle-based droplet generators with DLD technology can reduce droplet size variation by removing satellite droplets.[35,36] This combination offers the potential for high-throughput production of monodisperse droplets.

Achieving smaller droplet sizes presents additional challenges because it requires post-array miniaturization, which results in higher flow resistance and operating pressure. For example, Yeh *et al*. produced PLGA W/O droplets with a diameter of ~18 μm in diameter, which, while relatively small, remain larger than the few micrometer

droplets typically produced by mechanical homogenizers, suggesting potential limitations related to emulsion instability.[18] A key limitation is the pressure resistance of commonly used PDMS-glass bonding devices, which have a maximum leak pressure of 100–500 kPa.[37] In glass-Si or glass-glass microfluidic devices, bond strengths achieved through thermal annealing, low-temperature parylene-mediated bonding, and anodic bonding are approximately 20.7 MPa,[38] 7.6 MPa,[39] and 3.0 MPa,[40] respectively, offering up to a 41-fold increase in pressure resistance compared to PDMS-glass devices. Plastic devices fabricated via solvent-mediated bonding can also achieve high bond strengths (~ 18 MPa).[41] Transitioning from PDMS-glass to glass-based[42] or plastic-based[43] devices would therefore significantly enhance the pressure tolerance of post-array systems, enabling the generation of smaller droplets and improving their competitiveness with existing high-throughput emulsification methods.

III CONCLUSIONS AND OUTLOOK

In this study, we compared post-array devices with single-droplet splitting methods and various high-throughput droplet generators. The three main advantages of post-array devices are their shear-dependent tunability of droplet size, ease of high throughput capability, and resistance to clogging. Additionally, a unique feature of post-array devices is the influence of the dispersed phase fraction on droplet size, suggesting the potential for independent control of droplet size and dispersed phase fraction. These features make post-array devices particularly effective for applications where highly monodisperse droplets are not essential, but clogging resistance and high throughput are critical. For example, they are well suited for preliminary emulsification in double emulsification processes and biochemical analysis systems that accommodate droplets with high polydispersity.

By comparing post-array devices with other high-throughput droplet generation devices, we have clarified both their similarities and differences in droplet splitting behavior. However, several challenges remain. One major limitation is the variability in droplet size due to the stochastic nature of the breakup process. Another critical challenge is the need to further reduce the droplet size produced. Addressing these challenges will require both theoretical and experimental advances, including a deeper understanding of the droplet breakup mechanisms and improvements in the pressure resistance of the devices.

From a broader perspective, post-array devices can be viewed as a multiphase flow system operating within an interconnected channel network. This structural similarity is consistent with a number of seemingly unrelated fields, such as oil recovery in porous media.[44–46] Insights from these disciplines may inform further advances in post-array devices, while advances in post-array microfluidics may in turn provide valuable insights to other scientific and engineering domains.

ACKNOWLEDGMENTS

This work was supported by JSPS KAKENHI Grant Number 22J01188.

AUTHOR DECLARATIONS

Conflict of Interest

The authors have no conflicts to disclose.

Author Contributions

Shuzo Masui: Conceptualization (lead); formal analysis (lead); funding acquisition (lead); writing – original draft (lead). **Yusuke Kanno**: Formal analysis (supporting); writing – review and editing (supporting). **Takasi Nisisako**: Conceptualization (supporting); funding acquisition (supporting); supervision (lead); writing – review and editing (lead)

DATA AVAILABILITY

Data sharing is not applicable to this article as no new data were created or analyzed in this study.

REFERENCES

1. K. Schroen, C. Berton-Carabin, D. Renard, M. Marquis, A. Boire, R. Cochereau, C. Amine, and S. Marze, "Droplet microfluidics for food and nutrition applications," Micromachines **12**, 863 (2021).
2. D. Park, H. Kim, and J.W. Kim, "Microfluidic production of monodisperse emulsions for cosmetics," Biomicrofluidics **15**, 051302 (2021).
3. L. Zhang, R. Parvin, M. Chen, D. Hu, Q. Fan, and F. Ye, "High-throughput microfluidic droplets in biomolecular analytical system: A review," Biosens. Bioelectron. **228**, 115213 (2023).
4. F. Long, Y. Guo, Z. Zhang, J. Wang, Y. Ren, Y. Cheng, and G. Xu, "Recent progress of droplet microfluidic emulsification based synthesis of functional microparticles," Global Chall. **7**, 2300063 (2023).
5. L. Amirifar, M. Besanjideh, R. Nasiri, A. Shamloo, F. Nasrollahi, N.R. de Barros, E. Davoodi, A. Erdem, M. Mahmoodi, V. Hosseini, H. Montazerian, J. Jahangiry, M.A. Darabi, R. Haghniaz, M.R. Dokmeci, N. Annabi, S. Ahadian, and A. Khademhosseini, "Droplet-based microfluidics in biomedical applications," Biofabrication **14**, 022001 (2022).
6. L. Nan, H. Zhang, D.A. Weitz, and H.C. Shum, "Development and future of droplet microfluidics," Lab Chip **24**, 1135–1153 (2024).
7. L. Duan, W. Yuan, D. Liu, F. Chen, and J. Wei, "Active control of complex non-Newtonian polymer droplet formation in flow-focused microchannels by pulsatile flow," Chem. Eng. Sci. **309**, 121517 (2025).
8. L. Sheng, L. Ma, Y. Chen, J. Deng, and G. Luo, "A comprehensive study of droplet formation in a capillary embedded step T-junction: From squeezing to jetting," Chem. Eng. J. **427**, 132067 (2022).
9. J. Wu, S. Yadavali, D. Lee, and D.A. Issadore, "Scaling up the throughput of microfluidic droplet-based materials synthesis: A review of recent progress and outlook," Appl. Phys. Rev. **8**, 031304 (2021).

10. S. Rezvantalab, and M. Keshavarz Moraveji, "Microfluidic assisted synthesis of PLGA drug delivery systems," RSC Adv. **9**, 2055–2072 (2019).
11. I.C. Clark, and A.R. Abate, "Microfluidic bead encapsulation above 20 kHz with triggered drop formation," Lab Chip **18**, 3598–3605 (2018).
12. S.A. Byrnes, T.C. Chang, T. Huynh, A. Astashkina, B.H. Weigl, and K.P. Nichols, "Simple polydisperse droplet emulsion polymerase chain reaction with statistical volumetric correction compared with microfluidic droplet digital polymerase chain reaction," Anal. Chem. **90**, 9374–9380 (2018).
13. L. Chen, J. Ding, H. Yuan, C. Chen, and Z. Li, "Deep-dLAMP: Deep learning-enabled polydisperse emulsion-based digital loop-mediated isothermal amplification," Adv. Sci. **9**, 2105450 (2022).
14. H. Zhang, R. Gupte, Y. Li, C. Huang, A.R. Guzman, J.J. Han, H. Jung, R. Sabnis, P. de Figueiredo, and A. Han, "NOVAsort for error-free droplet microfluidics," Nat. Commun. **15**, 9444 (2024).
15. E. Amstad, S.S. Datta, and D.A. Weitz, "The microfluidic post-array device: high throughput production of single emulsion drops," Lab Chip **14**, 705–709 (2014).
16. S. Masui, Y. Kanno, and T. Nisisako, "Understanding droplet breakup in a post-array device with sheath-flow configuration," Lab Chip **23**, 4959–4966 (2023).
17. S. Akbari, T. Pirbodaghi, R.D. Kamm, and P.T. Hammond, "A versatile microfluidic device for high throughput production of microparticles and cell microencapsulation," Lab Chip **17**, 2067–2075 (2017).
18. S.-I. Yeh, C.-Y. Fu, C.-Y. Sung, and S.-C. Kao, "Microfluidic fabrication of porous PLGA microspheres without pre-emulsification step," Microfluid. Nanofluidics **27**, 47 (2023).
19. S. Yadavali, H.-H. Jeong, D. Lee, and D. Issadore, "Silicon and glass very large scale microfluidic droplet integration for terascale generation of polymer microparticles," Nat. Commun. **9**, 1222 (2018).
20. S.R. Derkach, "Rheology of emulsions," Adv. Colloid Interface Sci. **151**, 1–23 (2009).
21. R. Pal, "Novel viscosity equations for emulsions of two immiscible liquids," J. Rheol. **45**, 509–520 (2001).
22. A. Singla, B. Mehul, and B. Ray, "Droplet dynamics in a constricted microchannel," Chem. Eng. Sci. **300**, 120532 (2024).
23. D.R. Link, S.L. Anna, D.A. Weitz, and H.A. Stone, "Geometrically mediated breakup of drops in microfluidic devices," Phys. Rev. Lett. **92**, 054503 (2004).
24. X. Sun, C. Zhu, T. Fu, Y. Ma, and H.Z. Li, "Dynamics of droplet breakup and formation of satellite droplets in a microfluidic T-junction," Chem. Eng. Sci. **188**, 158–169 (2018).
25. A.M. Leshansky, and L.M. Pismen, "Breakup of drops in a microfluidic T junction," Phys. Fluids **21**, 023303 (2009).
26. M.-C. Jullien, M.-J. Tsang Mui Ching, C. Cohen, L. Menetrier, and P. Tabeling, "Droplet breakup in microfluidic T-junctions at small capillary numbers," Phys. Fluids **21**, 072001 (2009).

27. D.K. Deka, M.P. Boruah, S. Pati, P.R. Randive, and P.P. Mukherjee, "Tuning the splitting behavior of droplet in a bifurcating channel through wettability-capillarity interaction," Langmuir **36**, 10471–10489 (2020).
28. E. van der Zwan, K. Schroën, K. van Dijke, and R. Boom, "Visualization of droplet break-up in pre-mix membrane emulsification using microfluidic devices," Colloids Surf. A Physicochem. Eng. Asp. **277**, 223–229 (2006).
29. A. Nazir, and G.T. Vladisavljević, "Droplet breakup mechanisms in premix membrane emulsification and related microfluidic channels," Adv. Colloid Interface Sci. **290**, 102393 (2021).
30. A. Nazir, K. Schroën, and R. Boom, "High-throughput premix membrane emulsification using nickel sieves having straight-through pores," J. Memb. Sci. **383**, 116–123 (2011).
31. I. Kobayashi, M.A. Neves, Y. Wada, K. Uemura, and M. Nakajima, "Large microchannel emulsification device for mass producing uniformly sized droplets on a liter per hour scale," Green Process. Synth. **1**, 353–362 (2012).
32. S. Mashiyama, R. Hemmi, T. Sato, A. Kato, T. Taniguchi, and M. Yamada, "Pushing the limits of microfluidic droplet production efficiency: engineering microchannels with seamlessly implemented 3D inverse colloidal crystals," Lab Chip **24**, 171–181 (2024).
33. G.T. Vladisavljević, M. Shimizu, and T. Nakashima, "Production of multiple emulsions for drug delivery systems by repeated SPG membrane homogenization: Influence of mean pore size, interfacial tension and continuous phase viscosity," J. Memb. Sci. **284**, 373–383 (2006).
34. A. Hochstetter, R. Vernekar, R.H. Austin, H. Becker, J.P. Beech, D.A. Fedosov, G. Gompper, S.-C. Kim, J.T. Smith, G. Stolovitzky, J.O. Tegenfeldt, B.H. Wunsch, K.K. Zeming, T. Kruger, and D.W. Inglis, "Deterministic lateral displacement: challenges and perspectives," ACS Nano **14**, 10784–10795 (2020).
35. N. Tottori, T. Hatsuzawa, and T. Nisisako, "Separation of main and satellite droplets in a deterministic lateral displacement microfluidic device," RSC Adv. **7**, 35516–35524 (2017).
36. G. Ji, Y. Kanno, and T. Nisisako, "Microfluidic coupling of step emulsification and deterministic lateral displacement for producing satellite-free droplets and particles," Micromachines **14**, (2023).
37. A. Borók, K. Laboda, and A. Bonyár, "PDMS bonding technologies for microfluidic applications: A review," Biosensors **11**, 292 (2021).
38. E.F. Hasselbrink Jr, T.J. Shepodd, and J.E. Rehm, "High-pressure microfluidic control in lab-on-a-chip devices using mobile polymer monoliths," Anal. Chem. **74**, 4913–4918 (2002).
39. A.T. Ciftlik, and M.A.M. Gijs, "A low-temperature parylene-to-silicon dioxide bonding technique for high-pressure microfluidics," J. Micromech. Microeng. **21**, 035011 (2011).
40. N. Zhelev, T.S. Abhilash, R.G. Bennett, E.N. Smith, B. Ilic, J.M. Parpia, L.V. Levitin, X. Rojas, A. Casey, and J. Saunders, "Fabrication of microfluidic cavities using Si-to-glass anodic bonding," Rev. Sci. Instrum. **89**, 073902 (2018).

41. D.A. Mair, M. Rolandi, M. Snauko, R. Noroski, F. Svec, and J.M.J. Fréchet, "Room-temperature bonding for plastic high-pressure microfluidic chips," Anal. Chem. **79**, 5097–5102 (2007).
42. S. Aralekallu, R. Boddula, and V. Singh, "Development of glass-based microfluidic devices: A review on its fabrication and biologic applications," Mater. Des. **225**, 111517 (2023).
43. C.-W. Tsao, and D.L. DeVoe, "Bonding of thermoplastic polymer microfluidics," Microfluid. Nanofluidics **6**, 1–16 (2009).
44. D.G. Avraam, and A.C. Payatakes, "Flow regimes and relative permeabilities during steady-state two-phase flow in porous media," J. Fluid Mech. **293**, 207–236 (1995).
45. K.T. Tallakstad, H.A. Knudsen, T. Ramstad, G. Løvoll, K.J. Måløy, R. Toussaint, and E.G. Flekkøy, "Steady-state two-phase flow in porous media: statistics and transport properties," Phys. Rev. Lett. **102**, 074502 (2009).
46. S.S. Datta, J.-B. Dupin, and D.A. Weitz, "Fluid breakup during simultaneous two-phase flow through a three-dimensional porous medium," Phys. Fluids **26**, 062004 (2014).